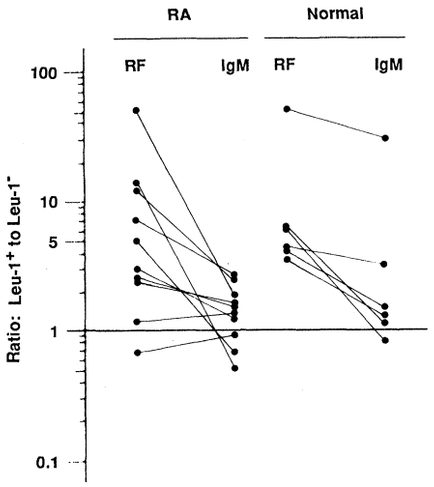

Fig. 3. Leu-1$^+$ B cells secrete a larger amount of RF than Leu-1$^-$ cells but secrete similar amounts of IgM. Data are the ratio of amounts secreted by Leu-1$^+$ B cells to that secreted by Leu-1$^-$ B cells from ten patients with rheumatoid arthritis and six control individuals determined as described in Table 1. Corresponding values from the same individual are connected by lines.

with cord blood and with PBLs from normal individuals [see also (*16*)].

Since our sorting experiments relied on depleting Leu-1$^+$ or Leu-1$^-$ cells that express B1, we verified (by depleting total B1$^+$ cells) that most of this SAC-induced RF secretion is derived from cells initially expressing the B1 (BP35, CD20) molecule. Therefore, our observations imply that RF secretion is derived from Leu-1$^+$ B cells even in cases where very few of these cells are present and that they are capable of high levels of RF secretion. Small amounts of secretion occasionally observed in a B1$^-$ fraction presumably resulted from preexisting terminally differentiated secreting cells (*17*). There remained the possibility that the enriched RF secretion observed in the Leu-1$^+$ fraction was caused by binding of the anti-Leu-1 staining reagent to B cell Fc receptors or to surface Ig (since RF cells are specific for IgG). However, in similar depletion-sorting experiments with mouse IgG2a control reagents unreactive with any human antigens, no significant enrichment (or depletion) in RF secretion was observed.

Our findings of enriched secretion of RF by a subpopulation of B cells has already been foreshadowed through fractionation of B cells by binding to mouse erythrocytes. Human B cells binding to mouse erythrocytes can be induced to secrete rheumatoid factor after Epstein-Barr virus stimulation (*18*). Moreover, chronic lymphocytic leukemia cells (which express Leu-1) also rosette with mouse erythrocytes (*19*), an indication that Leu-1$^+$ B cells may have been the source of RF in this earlier study. However, preliminary observations show that although such rosetting does enrich for Leu-1$^+$ B cells, it does not yield a pure population and therefore cannot be conclusive in assigning a functional role to these cells.

Our observations demonstrate that under the conditions we used, a particular subpopulation of B cells, which appears to be a separate lineage from Leu-1$^-$ B cells, is largely responsible for RF secretion. Although the significance of the increase in Leu-1$^+$ (or Ly-1$^+$) B cells in certain autoimmune diseases remains to be resolved, we might speculate that triggering to RF secretion would occur more readily in individuals with high levels of Leu-1$^+$ B cells, resulting in a predisposition to certain types of autoimmune diseases such as rheumatoid arthritis, Sjögren's syndrome, and progressive systemic sclerosis. It is intriguing that early in development, cells with features identical to this "autoimmune" population constitute a major fraction of B cells. The presence of a similar set of B cells in such a phylogenetically divergent species as the mouse suggests that these cells may have an important functional role and may provide a key to understanding the mechanism of antibody diversity in both mouse and man.

REFERENCES AND NOTES

1. L. Hang *et al.*, *J. Exp. Med.* **157**, 874 (1983).
2. K. Hayakawa *et al.*, *ibid.*, p. 202.
3. V. Manohar, E. Brown, W. M. Leiserson, T. M. Chused, *J. Immunol.* **129**, 532 (1982).
4. C. L. Sidman, L. D. Shultz, R. R. Hardy, K. Hayakawa, L. A. Herzenberg, *Science* **232**, 1423 (1986).
5. K. Hayakawa, R. R. Hardy, L. A. Herzenberg, L. A. Herzenberg, *J. Exp. Med.* **161**, 1554 (1985).
6. K. Hayakawa *et al.*, *Proc. Natl. Acad. Sci. U.S.A.* **81**, 2494 (1984).
7. L. A. Ledbetter *et al.*, *J. Exp. Med.* **153**, 310 (1981).
8. C. Y. Wang, R. A. Good, P. Ammirati, G. Dymbort, R. L. Evans, *ibid.* **151**, 1539 (1980).
9. F. Caligaris-Cappio, M. Gobbi, M. Bofill, G. Janossy, *ibid.* **155**, 623 (1982).
10. M. Bofill *et al.*, *J. Immunol.* **134**, 1531 (1985).
11. J. H. Antin *et al.*, *ibid.* **136**, 505 (1986).
12. K. A. Ault *et al.*, *J. Exp. Med.* **161**, 1483 (1985).
13. C. Plater-Zyberk, R. N. Maini, K. Lam, T. D. Kennedy, G. Janossy, *Arthritis Rheum.* **28**, 971 (1985).
14. H. Kikutani *et al.*, *J. Immunol.* **136**, 4019 (1986).
15. A. Forsgren, A. Svedjelund, H. Wigzell, *Eur. J. Immunol.* **6**, 207 (1976).
16. A. I. Levinson previously reported stimulation of RF secretion by SAC from both PBL and cord blood cells (*Proceedings of the 6th International Congress of Immunology*, Toronto, Canada, 6 to 11 July 1986, abstract 3.44, p. 22).
17. A. W. Boyd *et al.*, *J. Immunol.* **134**, 1516 (1985).
18. S. Fong, J. H. Vaughan, D. A. Carson, *ibid.* **130**, 162 (1983).
19. G. Stathopoulos and E. V. Elliott, *Lancet* **1974-I**, 600 (1974).

20. Supported by a grant-in-aid from the Japanese Ministry for Education, Science, and Culture.

12 February 1987; accepted 27 February 1987

Identification of Human Uromodulin as the Tamm-Horsfall Urinary Glycoprotein

DIANE PENNICA, WILLIAM J. KOHR, WUN-JING KUANG, DEBBIE GLAISTER, BHARAT B. AGGARWAL, ELLSON Y. CHEN, DAVID V. GOEDDEL

The primary structure of human uromodulin, a 616–amino acid, 85-kilodalton glycoprotein with in vitro immunosuppressive properties, was determined through isolation and characterization of complementary DNA and genomic clones. The amino acid sequence encoded by one of the exons of the uromodulin gene has homology to the low-density-lipoprotein receptor and the epidermal growth factor precursor. Northern hybridization analyses demonstrate that uromodulin is synthesized by the kidney. Evidence is provided that uromodulin is identical to the previously characterized Tamm-Horsfall glycoprotein, the most abundant protein in normal human urine.

UROMODULIN IS AN 85-KD GLYCOprotein isolated from the urine of pregnant women that is reported to be a potent immunosuppressive molecule (*1*). It inhibits antigen-induced T-cell proliferation and monocyte cytotoxicity in vitro at concentrations as low as 30 p*M* (*1*). Uromodulin has also been shown to be a high-affinity ligand for interleukin-1 (IL-1); it specifically inhibits a mouse thymocyte comitogenic assay dependent on IL-1 (*2*). The immunosuppressive activities of uromodulin are reported to reside predominantly in the N-linked carbohydrate residues of the protein (*2, 3*). Preliminary characterization of the purified protein revealed a very high carbohydrate content (~30%), a tendency to form aggregates, and the presence of intrachain disulfide linkages (*1*).

Another 85-kD polypeptide known as the Tamm-Horsfall glycoprotein (*4*) has many physical and biological characteristics in common with uromodulin. The Tamm-Horsfall glycoprotein is the most abundant protein of renal origin in normal urine and contains approximately 30% carbohydrate (*5*). The Tamm-Horsfall glycoprotein has also been found to have immunosuppressive

Departments of Molecular Biology and Developmental Biology, Genentech, Inc., South San Francisco, CA 94080.

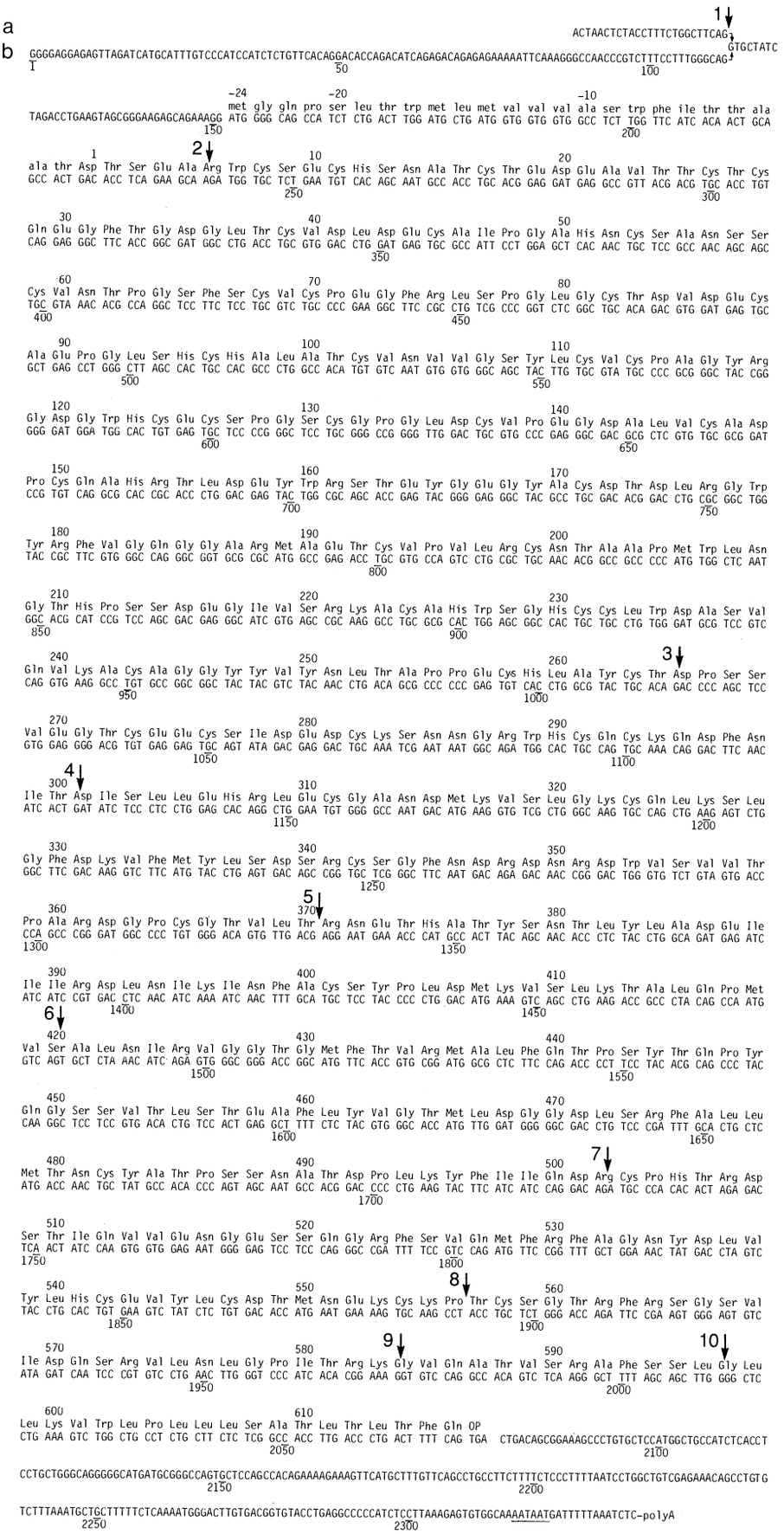

activities that are apparently localized to its carbohydrate moiety (*6–8*). We report here that uromodulin is in fact the previously described Tamm-Horsfall urinary glycoprotein.

Purified human uromodulin (*1*) was reduced and carboxymethylated and desalted by gel filtration. Aliquots of this preparation were treated with either trypsin or *Staphylococcus aureus* V8 protease. The sequences of some of the proteolytic fragments as well as the sequence of the NH_2 terminus of intact uromodulin were determined by automated protein sequence analysis (*9*). Deoxyoligonucleotide probes corresponding to six of the peptides and ranging from 33 to 54 nucleotides in length were chemically synthesized.

Since the site of synthesis of uromodulin was unknown, the strategy we pursued was to screen a human genomic DNA library for the uromodulin gene. Southern blots of human genomic DNA were hybridized with the six synthetic probes at low stringency and washed under gradually increased stringencies. When the washes were performed at 55°C with 0.5× SSC (standard saline citrate), probes B and C (*9*) hybridized to a single 2.3-kb Eco RI fragment. No hybridization signal was seen with the other four probes. Human DNA was digested with Eco RI, and the fragments from 2 to 3 kb were isolated and used to prepare a library of 200,000 clones in the vector λgt10. Twenty-seven clones were found to hybridize with probe C and five clones with probe B. None of the clones, however, hybridized with both probes, indicating that the sequences that hybridized with the two probes are on independent Eco RI fragments.

DNA sequence analysis demonstrated that the probe C–positive clones did not encode uromodulin. The DNA sequence of a 700-bp Sau 3A fragment from one of the probe B–positive clones (λD) revealed a match of 41 out of 48 positions with the

Fig. 1. Nucleotide sequence and deduced amino acid sequence of uromodulin cDNA. Nucleotides are numbered below each line, and amino acid positions are numbered above each line. The putative signal peptide is represented by the residues labeled −24 to −1; the predicted mature protein is numbered from 1 to 616. TGA at positions 2072–2074 indicates the translation stop codon. The putative polyadenylation signal AATAAT is underlined. The complete DNA sequence of the protein coding region of the uromodulin gene was also determined by sequencing the genomic clones described. The positions of introns were determined from genomic clone sequences and are indicated by arrows. The entire cDNA sequence was determined by the dideoxy chain termination method with restriction fragments subcloned into single-stranded M13 vectors (*32*). The a and b sequences denote the 5′ termini of cDNA clones λ33 and λ49, respectively (*33*).

probe. Furthermore, all 16 of the amino acids of the tryptic fragment from which probe B was designed were found encoded by this Sau 3A fragment. The entire 2.3-kb Eco RI fragment from the genomic clone λD was sequenced. Inspection of its largest open reading frame revealed matches with the amino acid sequence of eight additional uromodulin peptides derived from tryptic or staphylococcal V8 protease treatment as well as a portion of the NH_2-terminal sequence beginning with residue 7 of mature uromodulin. Only six amino acids from the NH_2-terminal sequence of mature uromodulin were not encoded by the λD Eco RI fragment. The presence in the gene sequence of a consensus splice site (*10*) in the sixth codon suggested that an intron interrupts the coding sequence at this point.

RNAs isolated from approximately 150 different epithelial, connective, and hematopoietic tissues and tumor-derived cell lines were screened for the presence of uromodulin messenger RNA (mRNA) with a 400-bp Bam HI–Pst I fragment isolated from the genomic clone λD. RNA from only one source, human adult kidney, hybridized to the probe. The size of this mRNA was determined to be approximately 2600 nucleotides. We constructed a λgt10 cDNA library using kidney poly(A)$^+$ mRNA and screened the library with the 400-bp Bam HI–Pst I probe and an NH_2-terminal synthetic oligonucleotide encoding the first 20 nucleotides of the coding exon of λD. When we used the Bam HI–Pst I probe, approximately 5% of the cloned complementary DNAs (cDNAs) gave a positive hybridization signal, suggesting that uromodulin mRNA is very abundant. The NH_2-terminal synthetic probe hybridized with approximately 1% of the cDNA clones. Three cDNA clones that hybridized with both probes were sequenced and found to encode all of the tryptic and staphylococcal V8 protease peptides as well as the mature NH_2 terminus of uromodulin (Asp-Thr-Ser-Glu-Ala . . .) in a single open reading frame (Fig. 1).

The uromodulin cDNA sequence determined from the three independent clones is 2352 bp in length. The open reading frame begins with the ATG at nucleotide positions 152 to 154 and extends for 1917 bp. The initiator methionine codon is followed by a sequence of 69 bp coding for a 23–amino acid signal peptide before the mature uromodulin sequence is encountered. There are 615 amino acids encoded after the NH_2-terminal aspartic acid of the mature protein. The molecular weight of the mature uromodulin polypeptide deduced from the amino acid sequence is 67,146. The TGA termination codon for uromodulin is followed by a

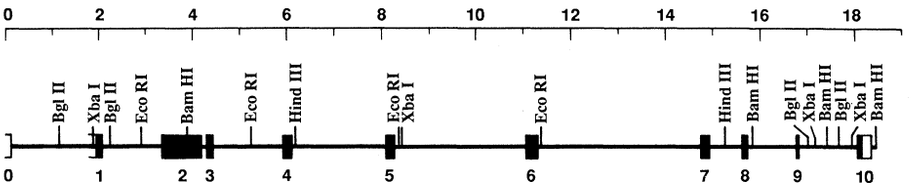

Fig. 2. Map of the human uromodulin gene. The structure of the uromodulin gene is schematically represented. The 11 exons are depicted as boxes and are drawn approximately to scale. The coding regions of the exons are indicated by shaded boxes, noncoding regions by open boxes. Restriction enzyme recognition sites for Bam HI, Bgl II, Eco RI, Hind III, and Xba I are shown. Additional sites for these enzymes may be present in unsequenced intron regions. The size scale in kilobases is indicated above the gene. The direction of transcription is from left to right.

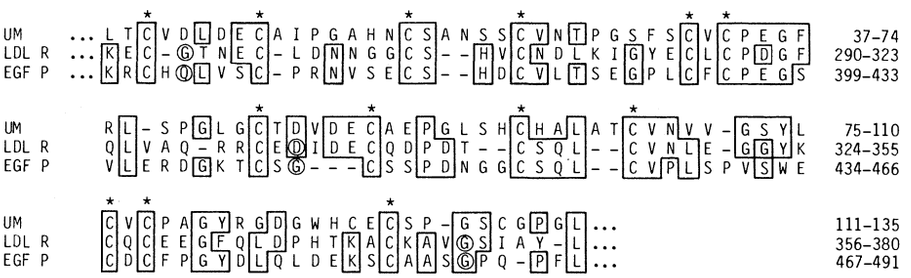

Fig. 3. Comparison of human uromodulin (UM), the human LDL receptor (LDL R), and human EGF precursor (EGF P) sequences (*19*). Amino acid residues that are identical in two of the three sequences are boxed. The numbering at the right indicates position in relation to the NH_2-termini. *, Cysteine residues. The positions at which introns interrupt the sequence are denoted by the encircled amino acids. The single-letter amino acid abbreviations are those recommended by the Commission on Biochemical Nomenclature (*34*).

260-bp 3′-untranslated region that contains the polyadenylation signal AATAAT (*11*) at positions 2317 to 2322.

Uromodulin contains an unusually high number of cysteine residues. Forty-eight cysteines give uromodulin the potential to be stabilized by 24 disulfide bridges. There are eight potential Asn-linked glycosylation sites (*12*) located at positions 14, 52, 56, 208, 251, 298, 372, and 489. This is consistent with the relatively high carbohydrate content (~30%) reported for uromodulin (*1*).

Another interesting feature of the uromodulin cDNA sequence is an unusually high proportion of CpG dinucleotides (*13*). Seventy-four of the CpG dinucleotides occur in exon 2. In this exon alone, the frequency of CpG pairs, if we take into account base composition and the expected CpG suppression (*14*), is four times as high as that occurring in most vertebrate DNA sequences. The existence of CpG clusters has also been seen in the polymorphic exons of major histocompatibility complex (MHC) genes and in the 5′ regions of the mouse dihydrofolate reductase (DHFR) gene and the chicken α2 collagen gene (*15*). In these genes, as also observed for uromodulin, there is an asymmetrical CpG distribution with more in the 5′ exons than in the 3′ exons. It has been suggested that these clusters are related to the absence of methylation at these regions in the germline and probably confer some significant structural feature to the DNA (*15, 16*).

A comparison of the uromodulin cDNA sequence with the genomic clone λD revealed that this 2.3-kb genomic Eco RI fragment contains two coding exons. The first is 777 bp in length and encodes amino acids 6 through 264 of the mature protein and the second exon is 108 bp and encodes amino acids 265 through 300. These two exons are separated by a small intron of 105 bp.

To find the remaining uromodulin genomic sequences, we screened a complete human genomic DNA library (*17*), using either the 400-bp Bam HI–Pst I fragment from the first exon of λD or a deoxyoligonucleotide (30mer) encoding amino acids 605 to 614 of the mature protein. Six different classes of overlapping clones, spanning approximately 20 kb of the human chromosome, were obtained. The restriction endonuclease map of the human uromodulin gene is depicted in Fig. 2. The DNA sequence of the 11 exons of the uromodulin gene represented in the cDNA clones was determined. The gene consists of ten coding exons ranging in size from 38 to 777 bp (~2.3 kb total) and at least one noncoding exon; the ten intron sizes range from 105 bp to approximately 3.5 kb (~16 kb total). Four nucleotide differences were found between the genomic and cDNA sequences, all of which are silent substitutions.

The NH_2-terminal region (amino acids 37 to 135) of uromodulin has significant

homology (*18*) to the human low-density lipoprotein (LDL) receptor (amino acids 290 to 380) and to the human epidermal growth factor (EGF) precursor (amino acids 399 to 491) (Fig. 3). In these regions, uromodulin is 33% homologous to the LDL receptor, 32% homologous to the EGF precursor, and 37% homology was observed between the LDL receptor and the EGF precursor (*19*). The homology between the LDL receptor and EGF precursor continues for an additional 300 amino acids in the COOH-terminal direction, whereas for uromodulin it diverges from the sequence of these two proteins after amino acid 135. For the structurally important amino acid cysteine, 13 residues can be aligned in the three proteins.

In the regions compared, three introns interrupt the coding sequence of both the LDL receptor and the EGF precursor in identical positions, whereas for uromodulin the homologous domain is entirely encoded within a single exon (exon 2). The similarity in intron positions between the EGF precursor and the LDL receptor has led to the suggestion that the homologous regions in these two genes arose by duplication of an ancestral gene (*19*). The different intron structure found in the uromodulin gene suggests that it may have evolved independently of the other two genes.

The significance of the structural homologies in the three proteins is difficult to determine. Uromodulin, the EGF precursor, and the LDL receptor have no obvious functional similarities. Structure-function relations of the LDL receptor have been studied extensively, but the function of this homologous domain has not been elucidated (*20*).

Uromodulin was originally described as a pregnancy-specific immunosuppressive glycoprotein (*1*). We obtained evidence suggesting that uromodulin may not be pregnancy-specific from a Northern blot of kidney mRNA isolated from male, female, and pregnant female rats. In all three samples, a 2.6-kb mRNA hybridized with approximately equal intensity to a human uromodulin cDNA probe. We next attempted to determine whether uromodulin could be purified from male or nonpregnant female human urine. Urine samples from a male, female, and pregnant female were dialyzed, concentrated, and subjected to SDS–polyacrylamide gel electrophoresis (SDS-PAGE) and NH_2-terminal sequence analysis. SDS-PAGE revealed a major polypeptide in all three urine samples that had an M_r of approximately 85,000 and comigrated with purified uromodulin (Fig. 4). Convincing evidence establishing the identity of this major urinary protein as uromodulin came from NH_2-terminal sequence data. The NH_2-terminal residues from this major protein in all three samples were identical to those of purified uromodulin. Our finding that uromodulin is not pregnancy-specific is supported by its recent detection in urine from males and nonpregnant females (*3*).

The most abundant protein in human urine has long been known as the Tamm-Horsfall glycoprotein (TH-GP) (*4, 5*). Approximately 15 to 37% of total urinary protein consists of this glycoprotein (*21*). First described in 1950 as an inhibitor of viral hemagglutination, the TH-GP is a normal constituent of human urine. It is synthesized by the kidney and localized in the cells lining the ascending limb of Henle's loop and the distal convoluted tubule (*22*). Up to 100 mg per day are excreted in healthy individuals, an amount apparently uninfluenced by age or sex (*23*). TH-GP may also be synthesized in the central nervous system since immunohistochemical studies on rat brain tissue sections have shown that ependymal cells and astrocytic processes react with antiserum to TH-GP (*24*).

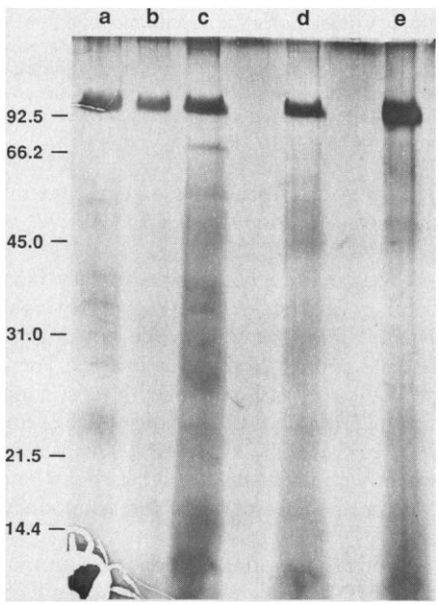

Fig. 4. SDS–polyacrylamide gel electrophoresis of human urine samples and purified uromodulin. Urine samples from a male, female, and pregnant female were collected and stored at 4°C. The urine was dialyzed against phosphate-buffered saline and concentrated by means of the reverse side of a YM10 Amicon filter membrane in a single step. The samples were concentrated approximately 23-, 27-, and 15-fold for the female, male, and pregnant female samples, respectively. Samples were separated by electrophoresis on a 10% SDS-polyacrylamide slab gel with the buffer system of Laemmli (*35*), and the gel was stained with silver stain (*36*). The far left of the figure indicates the position of migration of protein standards ($M_r \times 10^{-3}$): phosphorylase b (92.5), bovine serum albumin (66.2), ovalbumin (45.0), carbonic anhydrase (31.0), soybean trypsin inhibitor (21.5), and lysozyme (14.5). Lane a, male urine (52 ng); lane b, female urine (360 ng); lane c, pregnant female urine, concentrated only (500 ng); lane d, pregnant female urine concentrated and dialyzed (260 ng); and lane e, 1.5 μg of purified uromodulin (1.5 μg; *1*).

Some of the previously described chemical and physical characteristics of TH-GP (*5*) that closely resemble the properties described for uromodulin (*1–3*) include (i) an M_r estimated to be between 76,000 and 90,000, (ii) a unique tendency to form large aggregates of several million daltons in aqueous solution, (iii) the presence of 25 to 30% carbohydrate with a very high content of sialic acid, and (iv) an extremely high number of cysteine residues relative to other glycoproteins. Uromodulin has an M_r of 85,000, tends to aggregate in solution, contains 30% carbohydrate with 7 to 10% by weight sialic acid, and has 48 cysteine residues.

Consistent with the findings for uromodulin, TH-GP has also been found to have immunosuppressive activities (*6–8*). Both proteins inhibit antigen-induced proliferation of human lymphocytes. Certain oligosaccharides such as *N*-acetylgalactosamine can also block early events necessary for the expression of antigen-specific proliferation by human lymphocytes (*25*), but, as also observed for uromodulin, only if present during the first 24 hours of culture. In addition, the carbohydrate moieties of TH-GP have been characterized, and it has been found that *N*-acetylgalactosamine is the immunodominant sugar associated with this protein (*26*). Another common characteristic is that neither uromodulin, TH-GP, nor certain oligosaccharides have any effect on cell viability even after prolonged (6 to 7 days) incubation in vitro.

It has been suggested that the immunosuppressive activity of uromodulin resides solely in its carbohydrate moiety (*3*). Complete digestion of uromodulin with pronase or succinylation and carboxymethylation fail to inhibit its in vitro bioactivity. On the other hand, periodate treatment completely

Table 1. Amino acid composition of TH-GP and uromodulin.

Amino acid	Residues per 100 residues in protein	
	Tamm-Horsfall glycoprotein*	Uromodulin†
Asp + Asn	10.90	10.39
Thr	7.63	7.79
Ser	7.86	8.60
Glu + Gln	8.44	7.79
Pro	4.26	4.54
Gly	8.41	8.28
Ala	6.79	6.65
Val	6.40	6.65
Cys	8.41	7.79
Met	2.05	1.95
Ile	2.46	2.59
Leu	7.58	8.60
Tyr	3.83	3.57
Phe	3.14	3.25
Lys	2.65	2.59
His	2.67	2.43
Arg	4.49	4.87
Trp	1.68	1.62

*From (*37*). †Calculated from the actual 616–amino acid uromodulin sequence (see Fig. 1).

abolishes the immunosuppressive activity. Purified oligosaccharides from *N*-glycanase–digested uromodulin appear to be responsible for the majority of the in vitro immunosuppression. It is consistent with this information that the major glycopeptide fraction from TH-GP has also been found to be responsible for its immunosuppressive activity (*6, 7*). This inhibitory activity of TH-GP is thought to result from competition between the carbohydrate moiety of TH-GP and the carbohydrate receptor on lymphocytes for mitogens (*7*).

Uromodulin has also been found to inhibit in vitro assays dependent on IL-1, apparently by a specific high-affinity binding of uromodulin to IL-1 (*2*). The N-linked carbohydrate sequences are again implicated in this interaction based on the observations that deglycosylated uromodulin fails to bind IL-1 and that a partially purified oligosaccharide from uromodulin blocks the binding. On the basis of these results, Muchmore and Decker (*2*) have suggested that uromodulin may be a soluble form of the IL-1 receptor. Our failure to find uromodulin mRNA in any tissue except kidney argues against this possibility.

Although the physiological role of TH-GP is unknown, one suggestion is that it might be responsible for maintaining the water impermeability of the ascending limb by trapping water molecules, but allowing the passage of ions (*27*). TH-GP has been implicated as playing a role in a number of pathologic conditions. For example, cell-mediated and humoral responses directed against TH-GP have been demonstrated in patients with autoimmune liver disease and renal tubular acidosis (*28*). Autoantibodies to TH-GP have been found in patients with urinary tract infections (*29*), liver diseases (*30*), and hepatitis (*31*).

In summary, we have provided evidence to support our conclusion that uromodulin is identical to the previously characterized TH-GP. (i) Both are synthesized in the kidney and isolated from urine. (ii) The amino acid composition of uromodulin predicted by the DNA sequence closely fits the experimental data determined for the amino acid composition of the Tamm-Horsfall glycoprotein. (iii) Their NH_2-terminal amino acid residues are identical and so are most of the NH_2-terminal amino acids of their methionyl peptides. (iv) Both have similar M_r values, carbohydrate composition, an unusually high cysteine content, and a tendency to aggregate in solution. (v) Both possess in vitro immunosuppressive activities that appear to reside predominantly in the carbohydrate moiety of the proteins. Taken together, these data provide strong evidence that these two proteins are identical and probably do not function physiologically as immunosuppressive agents.

REFERENCES AND NOTES

1. A. V. Muchmore and J. M. Decker, *Science* **229**, 479 (1985).
2. ———, *J. Biol. Chem.* **261**, 13404 (1986).
3. A. V. Muchmore, S. Shifrin, J. M. Decker, *J. Immunol.*, in press.
4. I. Tamm and F. L. Horsfall, *Proc. Soc. Exp. Biol. Med.* **74**, 108 (1950); *J. Exp. Med.* **95**, 71 (1952).
5. A. P. Fletcher, in *Glycoproteins: Their Composition, Structure and Function*, A. Gottschalk, Ed. (Elsevier, New York, 1972), pp. 892–908.
6. C. F. Franceschi, F. Licastro, F. Chiricolo, F. Serafini-Cessi, P. Tabacchi, in *Lectins—Biology, Biochemistry, Clinical Biochemistry*, T. C. Bog-Hansen, Ed. (de Gruyter, Berlin, 1982), vol. 2, pp. 153–166.
7. A. Abbondanza, C. Franceschi, F. Licastro, F. Serafini-Cessi, *Biochem. J.* **187**, 525 (1980).
8. F. Serafini-Cessi, N. Malagolini, F. Dall'Olio, *Biosci. Rep.* **4**, 973 (1984); F. Serafini-Cessi, C. Franceschi, S. Sperti, *Biochem. J.* **183**, 381 (1979).
9. Tryptic digestion of reduced and carboxymethylated uromodulin was performed in 1% NH_4HCO_3 (*p*H 8.0) at 37°C for 18 hours with an enzyme-to-substrate ratio of 1:20. The digest was chromatographed on a Synchrom RP-4 column (4.6 mm by 10 cm). The elution solvents were 0.1% trifluoroacetic acid in water (solvent 1) and 1-propanol containing 0.07% trifluoroacetic acid (solvent 2). Elution was performed with a linear gradient from 1% solvent 2 and 99% solvent 1 to 50% of each solvent 1 and 2. Each peak was collected and rechromatographed on the same RP-4 column with acetonitrile containing 0.07% trifluoroacetic acid as solvent 2. *Staphylococcus aureus* V8 protease digestion of uromodulin was carried out in 0.1*M* tris (*p*H 8.0) with 0.1% Tween 20 at 37°C for 48 hours with two additions of *S. aureus* V8 protease at a 1:20 enzyme-to-substrate ratio for each addition. The digest was chromatographed on the same RP-4 column but elution solvent 1 was 0.1% triethylamine phosphate (*p*H 6.0) in H_2O and solvent 2 was 2.5 m*M* Quadrol (*p*H 9.0) in propanol. The isolated peptides were sequenced by a prototype gas-liquid phase sequencer with both trimethylamine and Quadrol as buffer and phenylisothiocyanate and trifluoroacetic acid as reagents. The NH_2-terminal sequence analysis was performed on both native and carboxymethylated uromodulin. The corresponding synthetic deoxyoligonucleotides used as probes for six of the peptide sequences are as follows: A, 5′ TTTGCTCCCAACTATGATCTGGTGTACCTG-CACTGTGAGGTGTACCTGCCTGAC; B, 5′ GC-CTGTGCTGGCGGCTATTATGTGTATAACCT-GACAGCCCCCCCTGAG; C, 5′ GAGGGGGAT-GCCCTGGTCTGTGCTGACCCATGCCAGGCT-GAG; D, 5′ TCTGCCCTGCAGATGACCAACTG-CTATGCCACCCCCCGG; E, 5′ GACACCTCT-GAGGCCCGGTGGTGCTCTGAGTGCCACTCC; and F, 5′ GAGGGCTATGCCTGTGACACAGA-CCTGCGGGGC.
10. R. Breathnach and P. A. Chambon, *Annu. Rev. Biochem.* **50**, 349 (1981); S. M. Mount, *Nucleic Acids Res.* **10**, 459 (1982).
11. M. Wickens and P. Stephenson, *Science* **226**, 1045 (1984).
12. P. J. Winzler, in *Hormonal Proteins and Peptides*, C. H. Li, Ed. (Academic Press, New York, 1973), pp. 1–15.
13. Taking into account base composition, the expected number of CpG dinucleotides in the coding region of uromodulin based on a random distribution would be 173. However, CpG dinucleotides are normally four to five times underrepresented in most mammalian genes (*14*) and therefore one would expect to find approximately 35 to 43 CpG sequences. The actual number of CpG pairs in uromodulin, 105, is about three times the predicted number.
14. M. Ehrlich and R. Y.-H. Wang, *Science* **212**, 1350 (1981).
15. M. L. Tykocinski and E. E. Max, *Nucleic Acids Res.* **12**, 4385 (1984).
16. A. Bird, M. Taggart, M. Frommer, O. J. Miller, D. Macleod, *Cell* **40**, 91 (1985).
17. R. M. Lawn, E. R. Fritsch, R. C. Parker, G. Blake, T. Maniatis, *ibid.* **15**, 1157 (1978).
18. These homologies are judged to be statistically significant on the basis of a comparison with the average homology found when the sequences are randomly permuted. This analysis gives *Z* values (the number of standard deviations from the mean random homology) of 13 for the LDL receptor and 6.4 for the EGF precursor [D. J. Lipman and W. R. Pearson, *Science* **227**, 1435 (1985)].
19. T. C. Südhof *et al.*, *Science* **228**, 893 (1985).
20. J. L. Goldstein *et al.*, *Annu. Rev. Cell Biol.* **1**, 1 (1985).
21. C. Lentner, in *Geigy Scientific Tables* (Medical Education Division, Ciba-Geigy Corporation, Summit, NJ, 1981), pp. 78–80.
22. E. A. Schenk, P. H. Schwartz, R. A. Lewis, *Lab. Invest.* **25**, 92 (1971); J. K. McKenzie and E. G. McQueen, *J. Clin. Pathol.* **22**, 334 (1969).
23. K. Lynn, *N.Z. Med. J.* **95**, 457 (1982).
24. B. Zalc *et al.*, *Brain Res.* **291**, 182 (1984).
25. A. V. Muchmore, J. M. Decker, R. M. Blaese, *J. Immunol.* **125**, 1306 (1980).
26. F. Serafini-Cessi and F. Dall'Olio, *Biochem. J.* **215**, 483 (1982).
27. K. L. Sikri, C. L. Foster, N. MacHugh, R. D. Marshall, *J. Anat.* **132**, 597 (1981).
28. D. C. Tsantoulas, I. G. McFarlane, B. Portman, A. L. W. F. Eddleston, R. Williams, *Br. Med. J.* **4**, 491 (1974).
29. R. Maurier *et al.*, *J. Infect. Dis.* **138**, 781 (1978); A. Fasth *et al.*, *Contrib. Nephrol.* **39**, 285 (1984); K. L. Lynn *et al.*, *ibid.*, p. 296.
30. A. Fasth, B. Kaijser, R. Olsson, *Allerg. Immunol.* **29**, 149 (1983).
31. V. Lindberg, A. Fasth, G. Norkrans, L. A. Nilsson, *Int. Archs. Allerg. Appl. Immunol.* **70**, 146 (1983).
32. F. Sanger, S. Nicklen, A. R. Coulson, *Proc. Natl. Acad. Sci. U.S.A.* **74**, 5463 (1977); C. Yanisch-Perron, J. Vieira, J. Messing, *Gene* **33**, 103 (1985).
33. Characterization of several cDNA clones revealed the existence of two distinct types of cDNAs whose sequence differs in a portion of their 5′-untranslated regions. The first type (represented by λ49) is colinear with the untranslated sequence presented in Fig. 1b. The second type of cDNA (Fig. 1a, represented by λ33) extends 39 bp 5′ of the initiator ATG before diverging from the first class of clones. These 22 bp of λ33 have been found about 2 kb upstream of the initiator ATG in the uromodulin genomic sequence, indicating that this alternative sequence is not a cloning artifact. Since the entire 5′-untranslated region of λ49 has also been found in the genomic DNA sequence, the different 5′ sequences of these two cDNAs have most likely arisen through alternate splicing of uromodulin mRNA.
34. M. O. Dayhoff, *Atlas of Protein Sequence and Structure*, suppl. 3 (National Biomedical Research Foundation, Washington, DC, 1978), vol. 5.

35. U. K. Laemmli, *Nature (London)* **227**, 680 (1970).
36. C. R. Merril, R. C. Switzer, M. L. Van Keuren, *Anal. Biochem.* **105**, 361 (1980).
37. A. P. Fletcher, A. Neuberger, W. A. Ratcliffe, *Biochem. J.* **120**, 417 (1970).
38. We thank A. Muchmore for providing the purified human uromodulin; A. Gray for providing the human kidney mRNA, T. Eessalu for performing the SDS-PAGE of the urine samples; C. Collins for help with DNA sequencing; P. Ng, P. Jhurani, and M. Vasser for preparation of synthetic deoxyoligonucleotides; R. Aiyer, P. Gray, and W. Wood for helpful discussions; and J. Arch for preparation of the manuscript.

14 November 1986; accepted 12 February 1987

Identification of an α Subunit of Dihydropyridine-Sensitive Brain Calcium Channels

MASAMI TAKAHASHI AND WILLIAM A. CATTERALL

Voltage-sensitive calcium channels in different tissues have diverse functional properties. Polyclonal antibodies (PAC-2) against the α subunits of purified rabbit skeletal muscle calcium channels immunoprecipitated calcium channels labeled with the dihydropyridine PN200-110 from both skeletal muscle and brain. The immunoreactivity of PAC-2 with the skeletal muscle channel was greater than that with the brain calcium channel and was absorbed only partially by prior treatment with the brain channel. PAC-2 specifically recognized a large peptide in synaptic plasma membranes of rabbit brain with an apparent molecular size of 169,000 daltons. This protein resembles an α subunit of the skeletal muscle calcium channel in apparent molecular weight, antigenic properties, and electrophoretic behavior after reduction of disulfide bonds. Thus, the dihydropyridine-sensitive calcium channel of rabbit brain has an α subunit that is homologous, but not identical, to those of the skeletal muscle calcium channel. The different functional properties of these two calcium channels may result from minor variations in structurally similar components.

THE VOLTAGE-SENSITIVE CALCIUM channel is one of the key factors in the control of calcium-linked cellular functions such as action-potential generation, muscle contraction, and secretion of hormones and neurotransmitters (*1*). In neurons, three different classes of Ca^{2+} channels have been described in electrophysiological experiments (*2, 3*). One of these, termed the L channel, mediates slowly activated, long-lasting Ca^{2+} currents that are blocked by dihydropyridine Ca^{2+} channel antagonists and enhanced by dihydropyridine Ca^{2+} channel agonists (*3*). Dihydropyridine-sensitive Ca^{2+} channels also mediate Ca^{2+} entry during the action potential in muscle tissues. High-affinity dihydropyridine receptors have been identified in skeletal, smooth, and cardiac muscles and in brain (*4*). They have been successfully solubilized (*5–8*) and purified to near homogeneity from skeletal muscle T-tubular membranes (*6, 9*). The purified dihydropyridine receptors consist of a noncovalent complex of α, β, and γ subunits having apparent molecular sizes of 160,000, 50,000, and 33,000 daltons, respectively (*6*). The apparent size of a fraction of the α subunits is reduced to 135,000 daltons by cleavage of disulfide bonds (*6, 10*). The purified dihydropyridine receptor from skeletal muscle has also been incorporated into phospholipid vesicles and bilayers and been shown to mediate dihydropyridine-sensitive Ca^{2+} conductance, which provides evidence that the three subunits are sufficient to mediate the physiological functions of the Ca^{2+} channel (*10*).

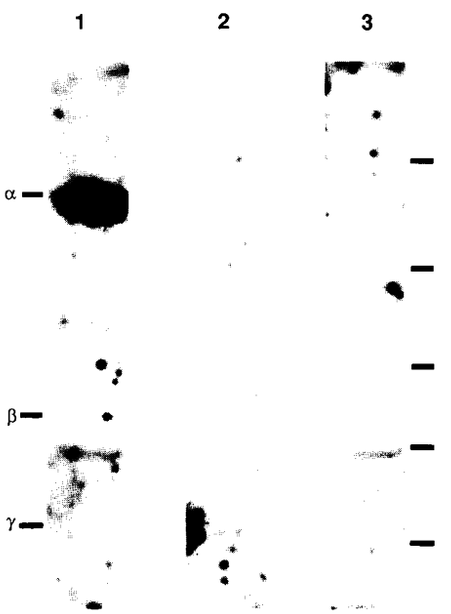

Fig. 1. Immunoblotting of T-tubule membranes from rabbit skeletal muscle by PAC-2. T-tubule membrane proteins (190 μg per lane) were transblotted from SDS–polyacrylamide gel to a nitrocellulose sheet and immunostained by PAC-2 (lane 1), preimmune serum (lane 2), and PAC-2 absorbed with purified rabbit skeletal muscle Ca^{2+} channel (lane 3). The concentrations of all the antisera were 0.3% by volume. The migration positions of α, β, and γ subunits of the skeletal muscle Ca^{2+} channel are indicated on the left. The migration positions of standard proteins indicated by horizontal bars correspond, from top to bottom, to the following molecular weights: 200,000, 116,000, 68,000, 42,000, and 30,000.

Although the Ca^{2+} channels of skeletal muscle T-tubules have served as a valuable model system for biochemical studies, Ca^{2+} channels in other tissues have many different properties. For example, dihydropyridine-sensitive Ca^{2+} channels in neurons have a higher affinity for dihydropyridine Ca^{2+} antagonists (*11*), high sensitivity to inhibition by ω-conotoxin (*12*), higher single-channel conductance (*3, 13*), faster kinetics of opening and closing (*2, 3, 14*), and different regulation by protein phosphorylation (*1, 10, 15*). In view of the importance of Ca^{2+} channels in neurons and the many functional differences between Ca^{2+} channels in neurons and skeletal muscle, it is of considerable interest to determine the molecular properties of dihydropyridine-sensitive Ca^{2+} channels in the brain. Here we describe polyclonal antibodies that recognize the α subunits of the purified skeletal muscle Ca^{2+} channel and use those antibodies to identify and compare a corresponding polypeptide component of the dihydropyridine-sensitive Ca^{2+} channels in the brain.

As a first step, we purified the brain dihydropyridine-sensitive Ca^{2+} channel by applying the methods used for T-tubule Ca^{2+} channels (*6*) (Table 1). The synaptic plasma membrane fraction purified from rabbit brain homogenate specifically bound 0.16 pmol of [^{3}H]PN200-110 per milligram of protein at saturation. Treatment with 1% digitonin solubilized 46% of the protein and 32% of the [^{3}H]PN200-110–channel complex (*5*). The solubilized channel was purified by chromatography on wheat germ agglutinin (WGA)–Sepharose and velocity sedimentation through a sucrose density gradient. The specific activity of final preparation was 2.91 pmol of [^{3}H]PN200-110 bound per milligram of protein, representing an overall 18.2-fold purification from the synaptic plasma membranes. If the molecular weight of dihydropyridine receptor in brain is 210,000 [as determined by radiation inactivation (*16*)], the specific activity of a homogeneous preparation would be 4760 pmol per milligram of protein, indicating that 1600-fold further purification is required to achieve homogeneity. Evidently the low concentration of dihydropyridine-sensitive Ca^{2+} channels in

Department of Pharmacology, School of Medicine, University of Washington, Seattle, WA 98195.